Role of Medium- and Short-Chain L-3-Hydroxyacyl-CoA Dehydrogenase in the Regulation of Body Weight and Thermogenesis

Schulz, N.; Himmelbauer, H.; Rath, M.; van Weeghel, M.; Houten, S.; Kulik, W.; Suhre, K.; Scherneck, S.; Vogel, H.; Kluge, R.; Wiedmer, P.; Joost, H.G.; Schürmann, A.

DOI
10.1210/en.2011-1547

Publication date
2011

Document Version
Final published version

Published in
Endocrinology

Role of Medium- and Short-Chain L-3-Hydroxyacyl-CoA Dehydrogenase in the Regulation of Body Weight and Thermogenesis

Nadja Schulz, Heinz Himmelbauer, Michaela Rath, Michel van Weeghel, Sander Houten, Wim Kulik, Karsten Suhre, Stephan Scherneck, Heike Vogel, Reinhart Kluge, Petra Wiedmer, Hans-Georg Joost, and Annette Schürmann

Department of Experimental Diabetology and Pharmacology (N.S., M.R., S.S., H.V., R.K., P.W., H.-G.J., A.S.), German Institute of Human Nutrition Potsdam-Rehbruecke, D-14558 Nuthetal, Germany; Max Planck Institute for Molecular Genetics (H.M.), 14195 Berlin, Germany; Center for Genomic Regulation and UPF (H.H.), 08003 Barcelona, Spain; Laboratory Genetic Metabolic Diseases (M.v.W., S.H., W.K.), Academic Medical Center, 1105 AZ Amsterdam, The Netherlands; Institute of Bioinformatics and Systems Biology (K.S.), Helmholtz Zentrum München, German Research Center for Environmental Health, D-85764 Neuherberg, Germany; and Department of Physiology and Biophysics (K.S.), Weill Cornell Medical College in Qatar, Education City, Qatar Foundation, Doha, Qatar

Dysregulation of fatty acid oxidation plays a pivotal role in the pathophysiology of obesity and insulin resistance. Medium- and short-chain-3-hydroxyacyl-coenzyme A (CoA) dehydrogenase (SCHAD) (gene name, *hadh*) catalyze the third reaction of the mitochondrial β-oxidation cascade, the oxidation of 3-hydroxyacyl-CoA to 3-ketoacyl-CoA, for medium- and short-chain fatty acids. We identified *hadh* as a putative obesity gene by comparison of two genome-wide scans, a quantitative trait locus analysis previously performed in the polygenic obese New Zealand obese mouse and an earlier described small interfering RNA-mediated mutagenesis in *Caenorhabditis elegans*. In the present study, we show that mice lacking SCHAD ($hadh^{-/-}$) displayed a lower body weight and a reduced fat mass in comparison with $hadh^{+/+}$ mice under high-fat diet conditions, presumably due to an impaired fuel efficiency, the loss of acylcarnitines via the urine, and increased body temperature. Food intake, total energy expenditure, and locomotor activity were not altered in knockout mice. $Hadh^{-/-}$ mice exhibited normal fat tolerance at 20 C. However, during cold exposure, knockout mice were unable to clear triglycerides from the plasma and to maintain their normal body temperature, indicating that SCHAD plays an important role in adaptive thermogenesis. Blood glucose concentrations in the fasted and postprandial state were significantly lower in $hadh^{-/-}$ mice, whereas insulin levels were elevated. Accordingly, insulin secretion in response to glucose and glucose plus palmitate was elevated in isolated islets of knockout mice. Therefore, our data indicate that SCHAD is involved in thermogenesis, in the maintenance of body weight, and in the regulation of nutrient-stimulated insulin secretion. **(*Endocrinology* 152: 4641–4651, 2011)**

Mitochondrial β-oxidation of fatty acids is vital for energy production, especially in periods of fasting and other metabolic stress. It occurs through a series of cyclic steps, in which fatty acids are catabolized to generate an acetyl-coenzyme A (CoA) and an acyl-CoA, which is two carbon units shorter (1). Patients have been identified with inherited disorders of mitochondrial β-oxidation with enzyme deficiencies at many of the steps in this pathway. Most defects, *e.g.* the medium-chain acyl-CoA dehydrogenase deficiency, which is the most common of

ISSN Print 0013-7227 ISSN Online 1945-7170
Printed in U.S.A.

doi: 10.1210/en.2011-1547 Received July 25, 2011. Accepted September 16, 2011.
First Published Online October 11, 2011

Abbreviations: BAT, Brown adipose tissue; CoA, coenzyme A; C4OH, hydroxybutyryl; C6OH, hydroxyhexanoylcarnitine; $FADH_2$, reduced flavin adenine dinucleotide; GAPDH, glyceraldehyde-3-phosphate dehydrogenase; HFD, high-fat diet; MS/MS, tandem mass spectrometry; NADH, reduced nicotinamide adenine dinucleotide; NZO, New Zealand obese; QTL, quantitative trait locus; SCHAD, short-chain-3-hydroxyacyl-CoA dehydrogenase; TEE, total energy expenditure; UPLC, ultraperformance liquid chromatography; VCO_2, carbon dioxide production; VO_2, oxygen consumption; UCP1, uncoupling protein 1.

the human acyl-CoA dehydrogenase deficiencies (1), are characterized by fasting-induced disease episodes of hypoketotic-hypoglycemia, metabolic acidosis, hyperammonemia, and fatty liver (2). Medium- and short-chain-3-hydroxyacyl-CoA dehydrogenase (SCHAD) catalyze the NAD^+-dependent conversion of L-3-hydroxyacyl-CoA to 3-ketoacyl-CoA and is highly expressed in heart, liver, adipose tissue, and in the islets of Langerhans within the pancreas (3). Patients with deficiency in SCHAD have hyperinsulinism, suggesting that a novel link between fatty acid oxidation and insulin secretion may explain hyperinsulinism in these patients (4). Up to now, SCHAD deficiency is the only disease in which a defective enzyme of the fatty acid β-oxidation is associated with increased insulin levels. Actually, Li *et al.* (5) confirmed this finding and demonstrated that mice lacking SCHAD ($hadh^{-/-}$ mice) exhibit reduced levels of plasma glucose and elevated levels of insulin, similar to children with SCHAD deficiency.

We identified the SCHAD-encoding gene *hadh* as potential obesity gene by comparing two screening approaches for putative obesity genes. In outcross populations of the New Zealand obese (NZO) mouse with lean mouse strains, we identified chromosomal segments [quantitative trait loci (QTL)] associated with adiposity (6–9). By positional cloning, we recently identified *Tbc1d1* in the obesity QTL *Nob1* that reduces fatty acid oxidation in muscle, thereby enhancing obesity and diabetes susceptibility (10). Several murine orthologs of *Caenorhabditis elegans* genes associated with altered fat storage (11) were located in the mouse adiposity QTL. These genes, like *hadh*, were considered strong candidates to be involved in the regulation of mammalian adiposity. Therefore, we further investigated the role of *hadh* for the energy homeostasis by deleting its gene in mice and characterizing their phenotype.

Here, we report that mice lacking *hadh* develop a slightly reduced body weight under a high-fat diet (HFD) due to an elevated body temperature. Furthermore, we confirm that SCHAD plays an important role in nutrient-dependent insulin secretion.

Materials and Methods

Generation of *hadh* knockout mice

For generation of *hadh* knockout mice, we used the gene-trap method. The gene-trap vector pGT0Lxf was inserted in the ES cell line E14Tg2a.4 (Bay Genomics, San Francisco, CA). The genomic background of the ES cells is 129P2/OlaHsd. ES cell clone RRM279 was injected into blastocysts, which were implanted into pseudopregnant females. Chimeras were mated with C57BL/6 mice, and F1 progeny carrying the transgene were backcrossed 6–10 times onto the C57BL/6 background. Genotyping of blastocysts, embryos, and mice was performed by PCR (forward primer for wild-type and knockout allele, 5′-TGC AGC TTG GCT TTG CTC CAC-3′ and reverse primer for wild-type allele, 5′-GCT CCT GCC CCA ACG AAA TCC-3′; for knockout allele, 5′-AGTATCGGCCTCAGGAAGATCG-3′). The animals were housed in air conditioned rooms (temperature 20 ± 2 C, relative moisture 50–60%) under a 12-h light, 12-h dark cycle. They were kept in accordance with United Kingdom legal requirements for the care and use of laboratory animals, and all experiments were approved by the ethics committee of the State Agency of Environment, Health and Consumer Protection (State of Brandenburg, Germany).

RNA preparation and first strand cDNA synthesis

Total RNA from liver, kidney, quadriceps, heart, and brown adipose tissue (BAT) and white adipose tissue was extracted with the TRIzol Reagent (Invitrogen, Carlsbad, CA) according to the guideline of the manufacturer. Extraction of total RNA from pancreas, stored in RNA*later*RNA Stabilization Reagent (QIAGEN, Hilden, Germany), was performed with RNeasy Mini kit (QIAGEN). cDNA was generated from 2 μg of total RNA with Superscript III and random hexamers as primers (Invitrogen). Quality of cDNA was controlled by PCR with murine glyceraldehyde-3-phosphate dehydrogenase (GAPDH) primers (forward, 5′-ACC ACA GTC CAT GCC ATC AC-3′; reverse, 5′-TCC CAC CAC CCT GTT GCT GTA-3′).

Quantitative real-time PCR

Quantitative real-time PCR analysis was performed with the Applied Biosystems 7500 Fast Real-time PCR System (Applied Biosystems, Foster City, CA). The PCR mix (10 μl) was composed of TaqMan Gene Expression PCR Master Mix, a cDNA amount corresponding to 12.5 ng of RNA used for cDNA synthesis (each sample in a triplicate), a fluorescence assay for the *hadh* mRNA, composed of a probe (5′-FAM-CAA AGA AGA AGT TCA CAG AAA ACC CTA AGG C-3′TAMRA), a forward primer (5′-GCA AAA TCC AAG AAG GGA ATT G-3′), and a reverse primer (5′-TGG TTG AAA GGC AGC TCA G-3′). The assay amplifies the region between exons 2 and 3, which is deleted in $hadh^{-/-}$ mice. For the determination of β-oxidation-related genes, SYBR Green Master Mix (Applied Biosystems) was used in combination with the primers for *Acadl* (forward primer, 5′-CAC TCA GAT ATT GTC ATG CCC T-3′; reverse primer, 5′-TCC ATT GAG AAT CCA ATC ACT C-3′), for *Acadm* (forward primer, 5′-GGC CAT TAA GAC CAA AGC AG-3′; reverse primer, 5′-AAT ATG TAT TCC CGG GGT GTC-3′), or for *Hadha* (forward primer, 5′-G GAA CAT TCG TGC AGA CAG-3′; reverse primer, 5′-GCT G AT CGG AAA GTC TCT GC-3′). Data were normalized referring to Livak and Schmittgen (12), whereas a β-actin self-made assay (probe, 5′-FAM-TTG AGA CCT TCA ACA CCC CAG CCA-3′TAMRA; forward primer, 5′-GCC AAC CGT GAA AAG ATG AC-3′; and reverse primer, 5′-TAC GAC CAG AGG CAT ACA G-3′) and mentioned primers for β-actin for the SYBR Green analysis, respectively, were used as endogenous control.

Immunochemical detection of SCHAD and CD36

For immunohistochemical detection of SCHAD, heart, liver, adipose tissues, and pancreas from $hadh^{+/+}$ and $hadh^{-/-}$ mice

were homogenized and centrifuged for 1 h at 200,000 × *g* at 4 C. Samples of 15 μg of protein/lane were separated by SDS-12% PAGE and transferred onto nitrocellulose. For immunochemical detection of SCHAD, an anti-SCHAD antibody (chicken, ab37673; Abcam, Cambridge, UK) was used in a dilution of 1:1000. For Western blot analysis of CD36, lysates of BAT were separated by SDS-PAGE and incubated with a CD36-specific antibody (rat) in a dilution of 1:500 (SR-B3; Research and Development, Minneapolis, MN). Bound immunoglobulines were conjugated with rabbit antichicken IgG (whole molecule, 1:20,000; Dianova, Hamburg, Germany) or goat antirat IgG (1:20,000; Pierce, Rockford, IL) antiperoxidase-conjugated antibodies and developed by enhanced chemiluminescence (Amersham Biosciences, Buckinghamshire, UK). For the detection of HADHA an anti-HADHA antibody (2 μg/μl, ab54477; Abcam) was used in combination with a secondary peroxidase-conjugated goat antirabbit antibody (1:20,000; Dianova). GAPDH (1:1000, AM4300; Ambion); α-tubulin (1:500, H-300; Santa Cruz Biotechnology, Inc., Santa Cruz, CA) or β-actin (1:10,000, a3853; Sigma, St. Louis, MO) were detected as loading control.

Diets

From the age of 3 wk, mice were fed either a normal maintenance diet (V153 × R/MH; Ssniff Spezialdiäten GmbH, Soest, Germany) containing 3.6 kcal/g energy with 23% (wt/wt) protein, 8% fat, and 69% carbohydrates or a HFD (D12492; Research Diets, Lane New Brunswick, NJ) containing 5.24 kcal/g energy with 20% (wt/wt) protein, 60% fat, and 20% carbohydrates.

Body composition

Body fat and lean mass were determined with a nuclear magnetic resonance spectrometer EchoMRI (Echo Medical Systems, Houston, TX). In addition, body weights were measured with an electronic scale (BP2100; Sartorius AG, Göttingen, Germany).

Serum parameters

Blood glucose levels were determined with an Accu-Chek glucometer (Roche Diagnostics GmbH, Mannheim, Germany). Cholesterol (CHOLESTEROL liquicolor; Human, Wiesbaden, Germany), triglycerides (Triyglyceride Reagent; Sigma), glycerol (Free Glycerol Reagent; Sigma), and nonesterified fatty acid (Wako nonesterified fatty acid C kit; Wako Chemicals, Neuss, Germany) were measured with the indicated kits, plasma insulin concentrations were determined by ELISA (insulin mouse ultrasensitive ELISA; DRG Instruments GmbH, Marburg, Germany).

Acylcarnitine measurements

Hydroxybutyryl (C4OH)- and hydroxyhexanoylcarnitine (C6OH)-carnitine concentrations in plasma were obtained by tandem mass spectrometry (MS/MS) analysis of butylated acylcarnitines (13, 14). Cardiac acylcarnitine levels were determined in freeze-dried tissue specimens as described previously (15). The concentrations of the stereo isomers of C4OH-carnitine were determined by ultraperformance liquid chromatography (UPLC) MS/MS based on principles described by Maeda *et al.* (16). In short, acylcarnitines were extracted using acetonitril, dried, reconstituted in the starting eluent, and stored at −20 C until analysis. Isomeric separation was achieved on a Acquity UPLC system (Waters, Milford, MA), equipped with an UPLC-BEH C18 column, 50 × 2.1 mm, 1.7-μm particle diameter (Waters), using a linear gradient of 0.1% heptafluorobutyric acid and methanol. A Quattro Premier XE triple quadrupole MS (Waters) was used in the positive electrospray ionization mode using the transition m/z 248.1 → m/z 85 for the detection of nonderivatized C4OH-carnitines. Using this method, we were able to detect baseline separated R- and S-3-C4OH-carnitine as well as other isobaric species in multiple matrices, such as urine and plasma. Identification of the compounds was performed using standards. As a proof of principle, plasma samples of SCHAD-deficient patients (S-3HB-carnitine), as well as type 1 diabetes mellitus patients presenting with ketoacidosis (R-3HB-carnitine), were analyzed for relative abundances of both stereo isomers.

Feeding behavior

Food intake was recorded with an automated Drinking & Feeding Monitor system (TSE, Bad Homburg, Germany), consisting of macrolon type III cages equipped with baskets connected to weight sensors. The baskets contained HFD pellets and were freely accessible to the mice. Mice were habituated to the test cages for 2 d before trials, and the measurement period lasted 2–3 d. Recorded data were analyzed as cumulative food intake.

Indirect calorimetry

Total energy expenditure (TEE) was measured by indirect calorimetry at 22 C for 24 h with an open circuitry calorimetry system (TSE). Before recoding the rates of oxygen consumption (VO_2) and carbon dioxide production (VCO_2), mice were allowed to adapt to the macrolon type II cage and to the system for 2 d. The air-tight respiratory cages were measured with a flow rate of about 0.38 l/min. VO_2 and VCO_2 were recorded for 1.5 min in 16-min intervals for each animal, so that three or four data points were obtained every other hour. TEE (kcal/h^{-1}) was calculated with the equation $TEE = 16.17/VO_2 + 5.03/VCO_2 - 5.98/N$, where N is excreted nitrogen and was assumed to be (0.1 g/d^{-1}).

Rectal body temperature

Rectal body temperature in wild-type and *hadh*$^{-/-}$ mice was measured with a rectal thermometer for mice (physitemp BAT-12; Physitemp Instruments, Clifton, NJ) when mice were resting.

Telemetric measurement of spontaneous locomotor activity

Transponders (22 × 8 mm; Mini Mitter Co., Inc., Bend, OR) were implanted into the abdominal cavity under ketamine (0.1 ml/kg body weight) and rompune (1.0 ml/kg body weight) anesthesia when the mice were at the age of 6 wk and weighed more than 20 g. The abdominal cavity was sutured with absorbable surgery thread (PGA Resorba; Resorba, Nürnberg, Germany), and skin was closed with metal clips (Becton Dickinson, Sparks, MD) that were removed after a 1-wk recovery period.

After a recovery period of 2 wk, spontaneous locomotor activity and body temperature data of single-housed mice were collected continuously for 48 h with the VitalView Data Acquisition System (Mini Mitter Co., Inc.) in macrolon type III cages. Values were recorded in 6-min intervals for each animal at 22 C.

Fat tolerance test

Ten-week-old overnight fasted mice received 10 μl/g body weight olive oil per gavage; 20 μl of blood samples were collected via the tail vein before (basal, time 0) and 2, 3, 4, 6, and 12 h after oral oil application for determination of plasma triglycerides, fatty acids, and cholesterol.

Cold tolerance test

For measuring cold tolerance, 11-wk-old male control and *hadh*$^{-/-}$ mice were housed singly in a macrolon type II cage for 3 h in a 4 C environment (2023 Minicold Lab; LKB, Bromma, Sweden). Rectal body temperature was taken before the experiment started and every 60 min. If the core body temperature of an animal decreased to 30 C, the experiment stopped for that mouse.

Isolation of islets of Langerhans

Control and *hadh*$^{-/-}$ mice (20 wk) kept under standard-diet conditions were killed by cervical dislocation. Through the open cavity, the common bile duct was clamped of the small intestine to inject 1 mg/ml collagenase P (Roche, Mannheim, Germany) directly in the pancreas. The inflated pancreas was transferred in a glass vial and digested for 7 min in a 37 C shaking water bath. After three washing steps, islets of Langerhans were hand picked in RPMI 1640 + L-glutamin (PAA, Laborbedarf, Austria). Thirty isolated islets were cultured for 72 h in 3-cm dishes with RPMI 1640 + L-glutamin in an 37 C, 5% CO_2, and 90% relative humidity incubator.

Glucose-stimulated insulin secretion

Isolated islets were starved for 1 h in Krebs-Ringer buffer containing 2.8 mM glucose and subsequently transferred in 2.8 mM glucose containing Krebs-Ringer buffer for 1 h followed by an incubation in 16.7 mM glucose for 1 h. Finally, islets were incubated in 35 mM KCl for 1 h. For measuring the additive effect of fatty acids, further experiments were performed in the presence of 0.3 mM palmitate. Insulin content was measured by ELISA and referred to the DNA-content (Quant-iT PicoGreen dsDNA; Invitrogen, Eugene, OR).

Detection of ketone bodies

Determination of ketone bodies in plasma was performed by the Autokit Total Ketone Bodies kit (Wako Chemicals) as described in manufacturer's instructions.

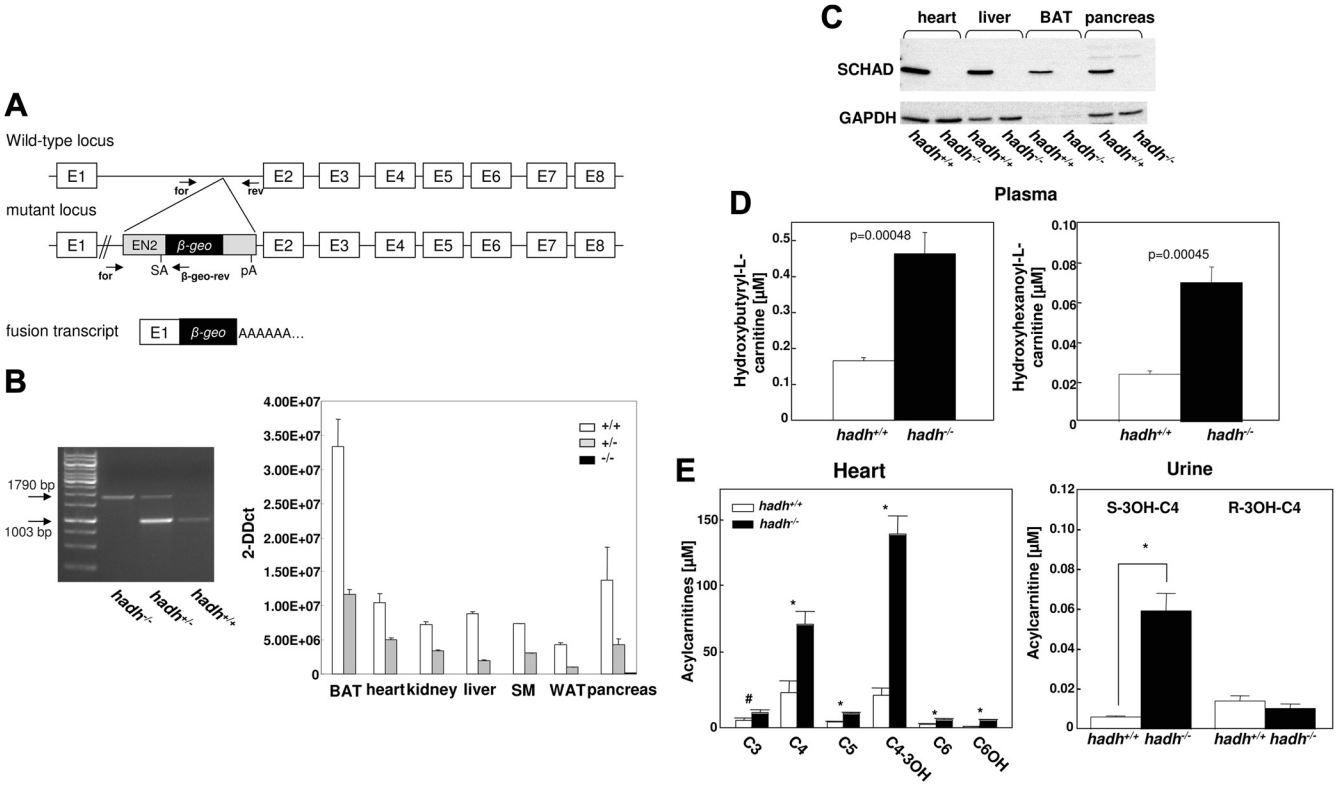

FIG. 1. Targeted disruption of the *hadh* gene by a gene-trap approach. A, Integration of a gene-trap sequence containing a splice acceptor site (SA), a β-geo cassette, and a polyadenylation signal (PA) in the first intron of the *hadh* gene resulted in a mRNA consisting of the sequence of the first exon and the a β-geo sequence. Primers used for genotyping are indicated. B, Genotyping of wild-type, heterozygous, and *hadh*$^{-/-}$ littermates was performed with specific primers by PCR on genomic DNA (*left panel*) as indicated in A. *Hadh* mRNA levels of 22-wk-old HFD-fed *hadh*$^{+/+}$, *hadh*$^{+/-}$, and *hadh*$^{-/-}$ littermates in BAT, heart, kidney, liver, skeletal muscle (SM), white adipose tissue (WAT), and pancreas were detected by quantitative RT-PCR as described in *Materials and Methods* (*right panel*). C, Western blot analysis of total membrane fractions from heart, liver, BAT, and pancreas of *hadh*$^{+/+}$ and *hadh*$^{-/-}$ littermates was performed with an anti-SCHAD antibody as described in *Materials and Methods*. An anti-GAPDH antibody was used as a loading control. D, Detection of C4OH-carnitine (*left panel*) and C6OH (*right panel*) in the plasma of *hadh*$^{+/+}$ and *hadh*$^{-/-}$ mice at the age of 11 wk. E, Concentration of short- and medium-chain acylcarnitines in extracts of hearts from *hadh*$^{+/+}$ and *hadh*$^{-/-}$ mice (*left panel*). Levels of (R)- and (S)-3-C4OH-carnitine in the urine of *hadh*$^{+/+}$ and *hadh*$^{-/-}$ mice (*right panel*). *, $P < 0.05$; #, $P < 0.01$.

Statistical analysis

Values are reported as mean ± SE. Statistical significance (P value less than 0.05) was determined by unpaired Student's t test.

Results

Targeted disruption of the *hadh* gene in mice

For the identification of putative obesity genes, we compared two genome-wide scans, which were performed in different species, a polygenic mouse model for the metabolic syndrome, the NZO mouse and the worm *C. elegans*. In outcross approaches of NZO with the lean Swiss/Jim Lambert or C57BL/6 mouse strains (6, 7, 9), we identified more than 10 obesity QTL located on different chromosomes. For the identification of novel obesity genes, we projected the orthologes of genes identified in a randomized screen in *C. elegans* (11) on the QTL map and identified more than 40 genes with an overlap. One of these genes, *hadh*, maps to the obesity QTL on chromosome 3 and encodes the enzyme medium- and short-chain-3-L-hydroxyacyl-CoA. To further test whether SCHAD plays a role in energy and/or glucose homeostasis, we generated *hadh* knockout mice by a gene-trap targeting strategy (Fig. 1A). Insertion of the gene-trap vector into intron 1 of *hadh* (Fig. 1A) resulted in a fusion protein consisting of 45 amino acids of SCHAD, neomycin phosphotransferase, and β-galactosidase. Male chimeric mice generated by injection of the gene-trap clone RRM279 into blastocysts were mated with C57BL/6 females, and F1 progeny carrying the transgene were backcrossed 6–10 times on to the C57BL/6 background. In the F2 progeny of heterozygous mice, we obtained the $hadh^{+/+}$, $hadh^{+/-}$, and $hadh^{-/-}$ mice (Fig. 1B, *left panel*) to the expected ratio (data not shown). To verify the knockout, RNA was isolated from different tissues of $hadh^{+/+}$, $hadh^{+/-}$, and $hadh^{-/-}$ mice, and *hadh* expression was analyzed by quantitative real-time PCR (Fig. 1B, *right panel*). *Hadh* expression was absent in all investigated tissues of $hadh^{-/-}$ mice, whereas tissues of heterozygous mice expressed approximately 50% of *hadh* (Fig. 1B, *right panel*). In addition, Western blot analysis of total membranes from heart, liver, BAT, and pancreas of $hadh^{+/+}$ and $hadh^{-/-}$ mice demonstrated the absence of the SCHAD protein in knockout mice (Fig. 1C).

To test whether other enzymes of the β-oxidation might compensate for the deleted *hadh*, the expression levels of *Acadl* (long-chain acyl-CoA dehydrogenase), *Acadm* (medium-chain acyl-CoA dehydrogenase), and *Hadha* (long-chain hydroxyacyl-CoA dehydrogenase) were quantified in liver of control and $hadh^{-/-}$ mice under fed (HFD) and fasted conditions. All three transcripts increased in response to fasting but did not differ between control and knockout livers (Supplemental Fig. 1A, published on The Endocrine Society's Journals Online web site at http://endo.endojournals.org). However, evaluating the protein content of HADHA in liver lysates by Western blotting clearly showed significantly higher levels in $hadh^{-/-}$ mice in comparison with the controls (Supplemental Fig. 1B). This effect was specific for liver and not detected in heart, skeletal muscle, BAT, and islets of Langerhans (Supplemental Fig. 1C).

To confirm that deletion of *hadh* results in a defective enzymatic activity of SCHAD, we performed metabolome analysis of plasma samples from $hadh^{+/+}$ and $hadh^{-/-}$ mice that were kept on the HFD and detected a specific increase of two acylcarnitines, C6OH- and C4OH-carnitine (Fig. 1D), whereas all other metabolites, amino acids, glycerophospholipids, and sphingolipids were not altered (data not shown). In addition, we measured the acylcarnitine profile in heart to prove the absence of SCHAD activity in tissues of $hadh^{-/-}$ mice. As demonstrated in Fig. 1E, *left panel*, we detected an accumulation of short-chain acylcarnitines such as of 3-C6OH in heart of $hadh^{-/-}$ mice. We analyzed urine samples of mice by the HPLC MS/MS (tandem mass spectrometry) method to distinguish between (R)- and (S)-3-C4OH-carnitine, the D- and L-isomer, respectively. Because SCHAD catalyzes specif-

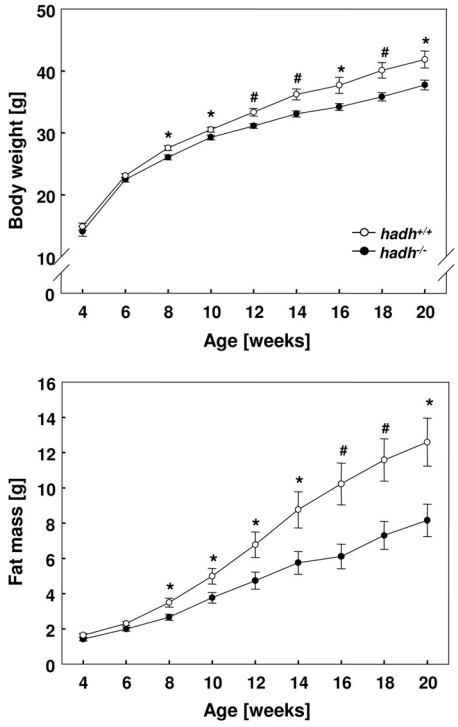

FIG. 2. Reduced body weight and body fat content in $hadh^{-/-}$ mice. Body weight development of male $hadh^{+/+}$ and $hadh^{-/-}$ mice fed a HFD (*upper panel*). Body fat mass of male $hadh^{+/+}$ and $hadh^{-/-}$ mice fed a HFD (*lower panel*). Data represent mean of 20 mice ± SE; *, $P < 0.05$; #, $P < 0.01$.

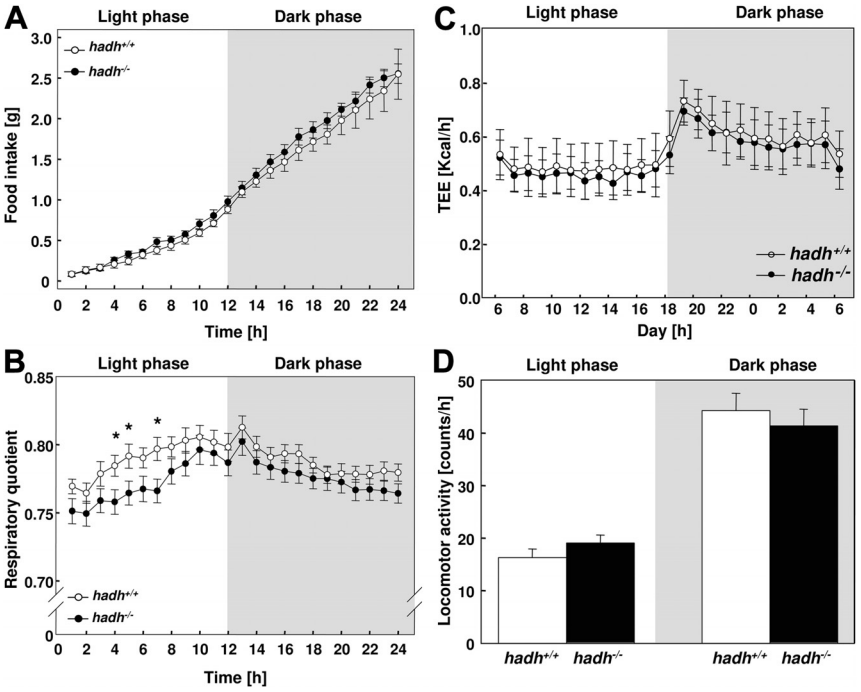

FIG. 3. *Hadh*$^{-/-}$ mice exhibit reduced RQ but normal energy expenditure. After weaning, male *hadh*$^{+/+}$ and *hadh*$^{-/-}$ littermates were fed a HFD, and (A) cumulative food intake (n = 11–14), (B) RQ (n = 12), (C) TEE as kcal per hour (n = 10), and (D) locomotor activity (n = 8–10) were measured at the age of 8 or 10 wk as described in *Materials and Methods*. Data represent mean ± SE; *, $P < 0.05$; #, $P < 0.01$.

ically the L-isomers, which are the β-oxidation intermediates, *hadh*$^{-/-}$ mice should only accumulate L-isomer. Indeed, *hadh*$^{-/-}$ mice accumulate only (S)-3-C4OH-carnitine, whereas no changes were detectable for (R)-3-C4OH-carnitine in urine of *hadh*$^{+/+}$ and *hadh*$^{-/-}$ mice (Fig. 1E, *right panel*).

Deletion of *hadh* reduces body weight and adipose tissue depots

Hadh$^{-/-}$ mice grew normally, were in an apparently good health, showed normal grooming and exploratory behavior, and exhibited no noticeable coat problems. We performed a broad characterization of the mice that were fed a standard diet and did not observe difference in body weight, body composition, and blood glucose concentrations (Supplemental Fig. 2). In contrast, on a HFD (60% of total calories from fat), male *hadh*$^{-/-}$ mice exhibited a significantly lower body weight gain over a period of 20 wk than their wild-type littermates (Fig. 2A). The reduced weight gain of *hadh*$^{-/-}$ mice was entirely due to reduced fat accumulation: knockout mice gained only 6.73 ± 0.81 g of body fat under the HFD, whereas wild-type mice gained 10.95 ± 1.26 g over a time period of 16 wk (Fig. 2B).

Higher lipid oxidation in *hadh*$^{-/-}$ mice

To study the main parameter of energy balance, we determined locomotor activity and body temperature at the age of 8 wk and daily food intake and TEE at the age of 10 wk in wild-type and *hadh*$^{-/-}$ mice fed with HFD. No significant differences in cumulative food intake were detected between *hadh*$^{-/-}$ and wild-type mice (Fig. 3A). To explore whether deletion of an enzyme involved in fatty acid oxidation affects the consumption of lipids, we conducted indirect calorimetry in 10-wk-old mice and determined the respiratory quotient (RQ). Interestingly, during the light period, the RQ was significantly lower in *hadh*$^{-/-}$ mice compared with *hadh*$^{+/+}$ mice (Fig. 2B), indicating higher fatty acid oxidation in mice lacking SCHAD. However, *hadh*$^{-/-}$ mice do not exhibit an alteration in energy expenditure (Fig. 3C) or locomotor activity (Fig. 3D) in comparison with wild-type littermates.

Impaired thermogenesis of *hadh*$^{-/-}$ mice

Because SCHAD is highly expressed in BAT, which itself is markedly enriched in mitochondria and the major site of facultative thermogenesis, we measured body temperature of control and *hadh*$^{-/-}$ mice that were kept at 20 C under HFD. As shown in Fig. 4A, *hadh*$^{-/-}$ mice exhibited significantly ($P < 0.05$) higher body temperature in both the light and the dark phase, which may contribute to the lower body weight of the *hadh*$^{-/-}$ mice (Fig. 2).

In BAT, fatty acid oxidation increases markedly during cold exposure (16). To generate heat and to maintain normal body temperature, ATP production is reduced when activated uncoupling protein 1 (UCP1) increases the flux of protons through the electron transport chain and dissipates the mitochondrial proton gradient (17). *Hadh*$^{+/+}$ mice can keep their body temperature between 35 and 36 C over 3 h at 4 C. In striking contrast, the body temperature of *hadh*$^{-/-}$ mice fell less than 32 C over that period, and we had to terminate the experiment (Fig. 4B). This difference was not associated with a reduced UCP1 expression as indicated in the Western blottings shown in Fig. 4C.

For the characterization of the lipid metabolism, we performed oral fat tolerance tests in HFD-fed mice. Approximately 2 h after oral application of olive oil, triglyceride concentrations increased and declined in the next 10 h back to basal levels. *Hadh*$^{-/-}$ mice showed the tendency toward lower triglyceride concentrations at each time point without reaching significance (area under the

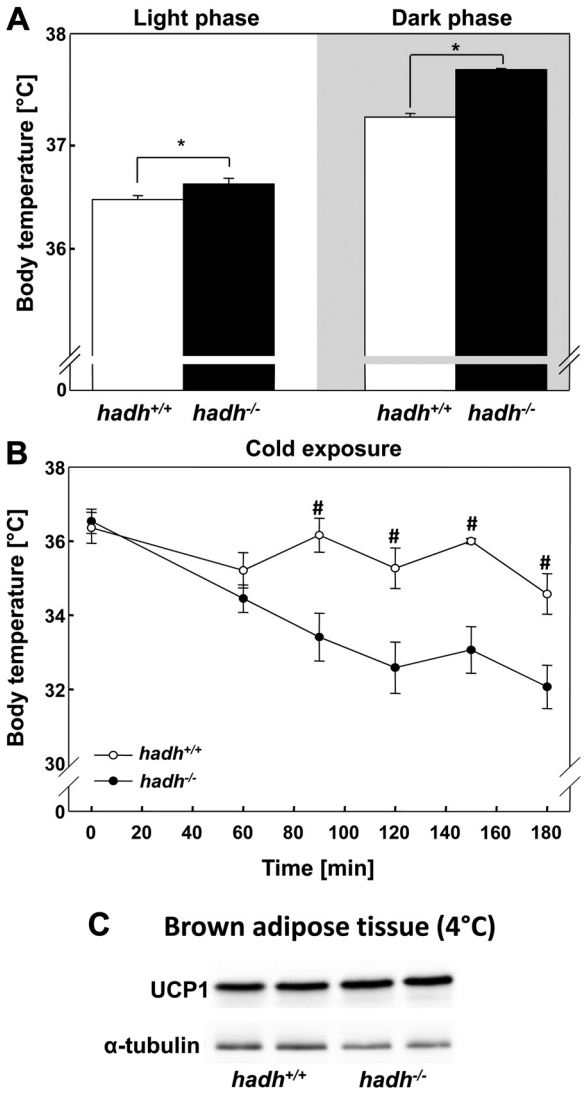

FIG. 4. Impaired thermogenesis of *hadh*$^{-/-}$ mice. A, Body core temperature of *hadh*$^{+/+}$ and *hadh*$^{-/-}$ mice kept at 20 C (n = 8–10) on a HFD. B, Body temperature of *hadh*$^{+/+}$ and *hadh*$^{-/-}$ mice that were kept at 4 C (n = 5–10). C, Western blottings of lysates of BAT from *hadh*$^{+/+}$ and *hadh*$^{-/-}$ mice were analyzed with an anti-UCP1 antiserum. An antibody against α-tubulin was used as loading control. *, $P < 0.05$; #, $P < 0.01$.

curve for *hadh*$^{+/+}$ mice, 12010 ± 1924 and for *hadh*$^{-/-}$ mice, 8835 ± 2639; $P = 0.433$). In addition, concentrations of free fatty acids showed similar changes with highest levels between 3 and 4 h after oil application in both *hadh*$^{+/+}$ and *hadh*$^{-/-}$ mice (Fig. 5A). Significant differences in fat tolerance were detected when mice were kept at 4 C. *Hadh*$^{+/+}$ mice show only a moderate increase in the concentration of plasma triglycerides and fatty acids in comparison with the levels detected under conditions of 20 C. This difference likely indicates that *hadh*$^{-/-}$ mice might not be able to accelerate triglyceride clearance. In contrast to this, *hadh*$^{-/-}$ mice show significantly higher triglyceride and free fatty acid concentrations at 4 C (Fig. 5B), indicating that they are not able to accelerate triglyceride clearance. To test whether impaired triglyceride clearance is the result of a defective fatty acid uptake into BAT, we studied expression of the fatty acid transporter CD36 in this fat depot of mice kept at room temperature or at 4 C. As shown in Supplemental Fig. 3, we detected higher CD36 protein levels after cold exposure than at 22 C. However, the CD36 levels did not differ between *hadh*$^{+/+}$ and *hadh*$^{-/-}$ mice.

Ketone bodies are generated as by-products of fatty acid oxidation from acetyl-CoA primarily in the liver, for instance in the fasted state, when glucose concentration is very low. To test whether the levels of ketone bodies differs between *hadh*$^{+/+}$ and *hadh*$^{-/-}$ mice, we determined their plasma concentrations in the fed and fasted state as well as after cold exposures. As expected, the concentration was low in the fed state and increased in response to fasting (Supplemental Fig. 4). However, we did not detect differences in the concentration of ketone bodies between control and *hadh*$^{-/-}$ mice under these conditions. Interestingly, the ketone body content increased at 4 C to the same level as after overnight fasting period in control mice, whereas *hadh*$^{-/-}$ mice showed significantly lower levels than control mice (Supplemental Fig. 4). This effect might be the consequence of the impaired triglyceride clearance and participate in the impaired thermoregulation of *hadh*$^{-/-}$ mice.

Elevated insulin secretion in response to glucose and fatty acids

In addition to the reduced body weight, a second striking phenotype of the HFD-fed *hadh*$^{-/-}$ mice was the lower blood glucose concentration in comparison with control mice. When randomly measured, after fasting or after fasting and a subsequent 2-h refeeding period, glucose concentrations of *hadh*$^{-/-}$ mice were significantly lower than in the corresponding control animals (Fig. 6A). The corresponding plasma insulin concentrations showed only a significant difference in the postprandial state, they were higher in *hadh*$^{-/-}$ mice than in *hadh*$^{+/+}$ mice (Fig. 6B), indicating that the nutrient-mediated insulin secretion is higher in the absence of SCHAD. To study this in more detail, we isolated islets from *hadh*$^{+/+}$ and *hadh*$^{-/-}$ mice that were kept on a standard diet and measured insulin secretion at 2.8 and 16.7 mM glucose or at 2.8 mM glucose plus 35 mM KCl alone or in the presence of 0.3 mM palmitate. Insulin secretion increased with increased glucose concentrations, and the supplementation of palmitate showed additive effects as described (18). As expected from insulin levels in the postprandial state (Fig. 6B) and from the phenotype of patients with SCHAD deficiency who suffer from hyperinsulinism, insulin secretion of iso-

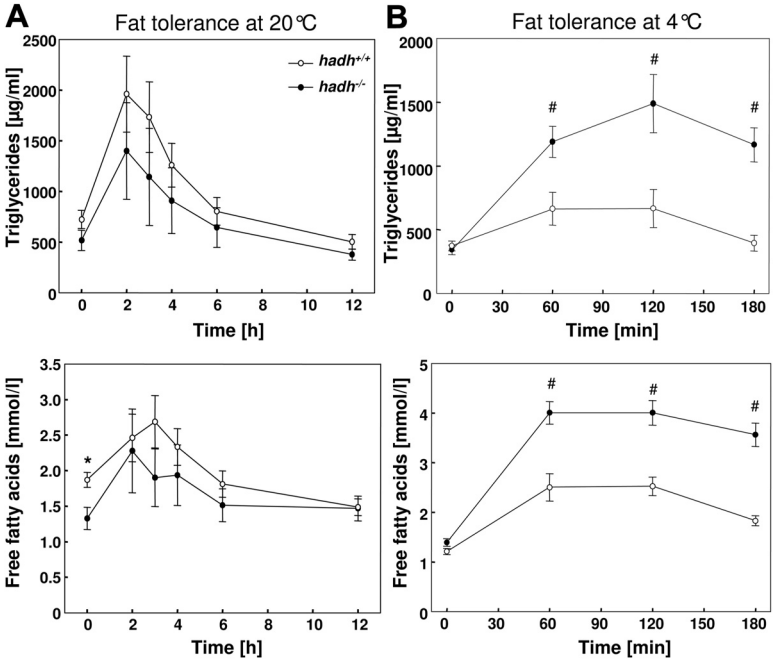

FIG. 5. Impaired triglyceride clearance of *hadh*$^{-/-}$ mice under cold exposure. Oral fat tolerance tests were performed as described in *Materials and Methods* with HFD-fed *hadh*$^{+/+}$ and *hadh*$^{-/-}$ mice that were kept at 20 C (A) or acutely put to 4 C (B). Mice that were fasted overnight, received an oral olive oil bolus, and concentrations of plasma triglycerides (*upper panels*) and free fatty acids (*lower panels*) were detected at the indicated time points. Data represent means of 7–14 mice ± SE. *, $P < 0.05$; #, $P < 0.01$.

lated islets of *hadh*$^{-/-}$ mice was higher at 16.7 mM glucose (Fig. 6C).

Discussion

SCHAD is a mitochondrial enzyme that catalyzes the penultimate reaction in β-oxidation. Genetic deficiency of *hadh* is associated with elevated plasma insulin levels, enhanced excretion of L-3-hydroxyglutarate in the urine, and increased L-3-C4OH-carnitine concentrations in the blood (19). We identified the SCHAD-encoding gene *hadh* as putative obesity gene and could indeed demonstrate that mice lacking *hadh* gene were protected from diet-induced obesity because of reduced fuel efficiency, lower RQ, as well as an elevated body temperature.

We explain the reduced body weight and fat mass of *hadh*$^{-/-}$ mice (Fig. 2) by two effects: the loss of acylcarnitines via the urine (Fig. 1E) (1) and the increased body temperature (Fig. 4A) (2). The fact that the RQ of *hadh*$^{-/-}$ mice is reduced (Fig. 3B) indicates that they consume more oxygen in relation to VCO_2. The theoretic calculation of the VO_2 and the VCO_2 of control mice that digest palmitate results in a ratio of 23:16 revealing a RQ of 0.7. However, *hadh*$^{-/-}$ mice are not able to metabolize palmitate completely, the reaction stops on the level of 3-L-C4OH-CoA (Fig. 1D), employing 18.5 molecules of oxygen and generating 12 molecules of carbon dioxide, which results in a RQ of 0.65. The incomplete digestion of fatty acids and the excretion of 3-L-C4OH-CoA via the urine in the absence of SCHAD implicate an elevated consumption of glucose, amino acids, and fatty acids to generate comparable levels of energy in form of ATP. The complete metabolism of one molecule of palmitate generates 106 molecules of ATP, whereas the incomplete reaction of *hadh*$^{-/-}$ mice only provides 78 molecules of ATP. Actually, we detect lower blood glucose concentrations under different conditions (Fig. 6A) and lower levels of triglycerides and free fatty acids in the fasted state of *hadh*$^{-/-}$ mice as detected in the fat tolerance tests (Fig. 5). Interestingly, the phenotypes of the *hadh*$^{-/-}$ mice were specifically detected under HFD conditions, which means, when triglycerides were the main source of energy. Thus, we do not believe that β-oxidation is totally disrupted in the absence of SCHAD, but that it is interrupted in one of the latest steps, which results in the accumulation and excretion of acylcarnitines. According to the fact that the cells and organs need ATP for their energy demand, more fatty acids have to be oxidized up to the step of hydroxyglutarate and C4OH-carnitine.

Body temperature in knockout mice is elevated under normal conditions (20 C) (Fig. 5A), which may also result in an elevated energy demand. Why is the body temperature of the *hadh*$^{-/-}$ mice higher? According to the lack of SCHAD, we expect that the consumption of palmitate generates seven reduced flavin adenine dinucleotide ($FADH_2$) and six reduced nicotinamide adenine dinucleotide $(NADH)^+ + H^+$ (wild-type cells generate seven $FADH_2$ and seven $NADH^+ + H^+$ per palmitate), because NAD^+ is reduced to $NADH^+ + H^+$ in the SCHAD-mediated conversion of L-hydroxyacyl-CoA to 3-ketoacyl-CoA (Fig. 7). The bisection of electron donors in *hadh*$^{-/-}$ cells would indicate a limited capacity of heat production by uncoupling. However, as stated above, *hadh*$^{-/-}$ mice have to burn more fat to generate similar levels of ATP. We therefore assume that this finally results in the generation of additional reduction equivalents and in higher body temperature. However, the difference in body temperature is very moderate (0.4 C) and therefore not detectable by an elevated energy expenditure, as we recently determined for the *Abcg1*$^{-/-}$ mouse. This model had a 1 C higher body temperature than the wild-type littermates, an effect that associated with slightly higher energy expen-

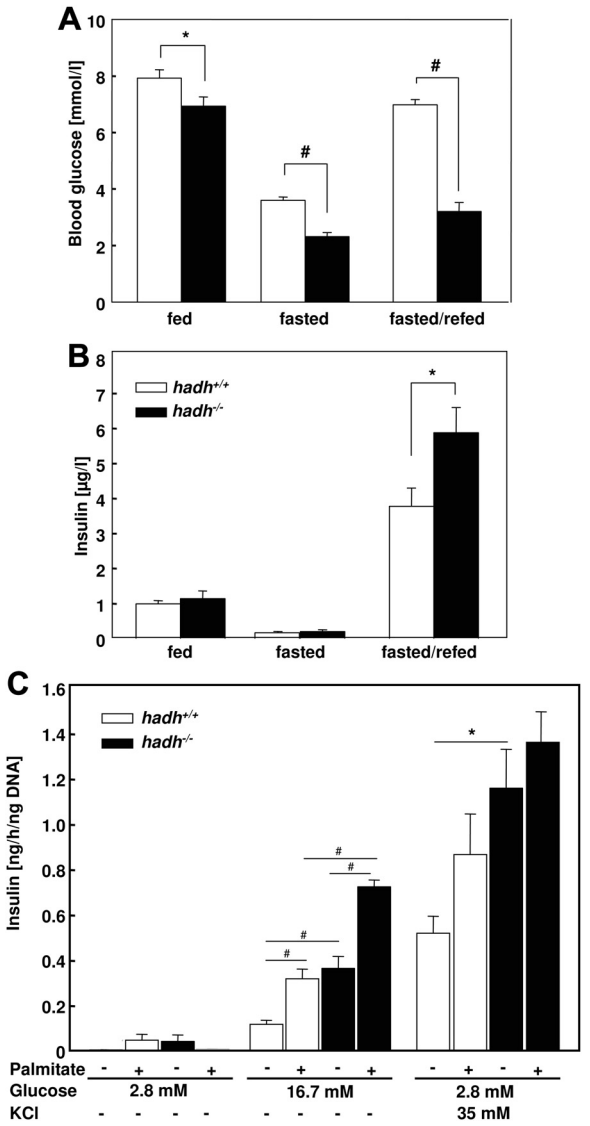

FIG. 6. Elevated insulin secretion of *hadh*$^{-/-}$ mice. Blood glucose (A) and plasma insulin (B) concentrations of *hadh*$^{+/+}$ and *hadh*$^{-/-}$ mice in the fed, fasted, and postprandial state (16-h fasting and 2-h access to diet). Data represent means of 12–16 mice ± SE; *, $P < 0.05$; #, $P < 0.001$. C, Elevated insulin secretion of isolated islets from *hadh*$^{-/-}$ mice in response to glucose and fatty acids. Islets of *hadh*$^{+/+}$ and *hadh*$^{-/-}$ mice that were kept on a standard diet were isolated as described in *Materials and Methods*. After an overnight incubation in RPMI medium islets were incubated with 2.8 or 16.7 mM glucose, with 2.8 mM glucose plus 35 mM KCl alone or in the presence of 0.3 mM palmitate for 1 h. Insulin secreted by the islets was detected in the medium by an ELISA as described in *Materials and Methods*; *, $P < 0.05$; #, $P < 0.01$.

diture and reduced body weight (20). We assume that the measurement of energy expenditure by indirect calorimetry is not sensitive enough to detect the moderately increased body temperature of the *hadh*$^{-/-}$ mouse.

In contrast, *hadh*$^{-/-}$ mice are, like other mice lacking enzymes of the β-oxidation, cold intolerant (1, 21, 22). Our data indicate that *hadh*$^{-/-}$ mice are unable to clear the lipids from the plasma when they are exposed to 4 C (Fig.

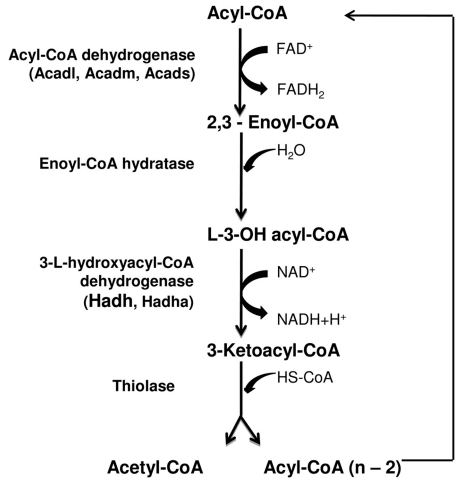

FIG. 7. Schematic demonstration of mitochondrial fatty acid β-oxidation and the enzymes catalyzing the different steps. Acadl, Long-chain acyl-CoA dehydrogenase; Acadm, medium-chain acyl-CoA dehydrogenase; Acads, short-chain acyl-CoA dehydrogenase; Hadh, medium- and short-chain hydroxyacyl-CoA dehydrogenase; Hadha, long-chain hydroxyacyl-CoA dehydrogenase.

6). Therefore, a reduced cleavage of triglycerides and/or uptake into the BAT appears to be responsible for drop of the body temperature in the absence of SCHAD, and we hypothesize that metabolites, such as C4OH-carnitine, mediate these effects. Similarly, mice lacking the transmembrane lipid and lipoprotein receptor CD36 exhibit elevated free fatty acid concentrations after cold exposure and are cold intolerant (16). The mechanisms described above, resulting in elevated body temperature of *hadh*$^{-/-}$ mice under control conditions (20 C), are obviously insufficient to facilitate adaptive thermogenesis.

Another striking effect of SCHAD deficiency was the reduced blood sugar concentration under control, fasted, and postprandial conditions (Fig. 6A). This could be a secondary effect of the inefficient fuel consumption of *hadh*$^{-/-}$ mice (see above). However, in the postprandial state, the reduced blood glucose levels can be explained by elevated plasma insulin concentrations (Fig. 6B). According to this, glucose-stimulated insulin secretion was higher in isolated islets of *hadh*$^{-/-}$ mice than in that of control mice (Fig. 6C). In addition, the additive effect of fatty acids on insulin release (19) was higher in *hadh*$^{-/-}$ islets. This finding confirms effects of SCHAD deficiency detected in humans. Children with mutations in *HADH* gene suffer from nonketonic and hypoglycaemic hyperinsulinemia (4, 19, 23). However, our observation is in contrast to that of Li *et al.* (5), who detected insulin release from perifused islets and observed a hypersensitivity of *hadh*$^{-/-}$ islets to amino acid-stimulated insulin secretion but no changes in response to glucose (5). One reason for this difference might be the genetic background (24) of the knockout mice; for our studies, we used mice that were backcrossed

6–10 times with C57BL/6 mice, whereas no backcrossing was mentioned in Li *et al.* (5), indicating that those mice had a mixed background of NIH Black Swiss and C57BL/6. The two most prominent examples for differences in the phenotype of one mutation on two different genetic backgrounds are the leptin gene (ob/ob) and the leptin receptor gene (db/db). Both loss-of-function mutations produce massive obesity on the B6 and the BKS (C57LBKS/J) background. However, on the BKS background, both mutations produced a life-shortening diabetes, whereas mice on the B6 background were normoglycemic (24–26). Another reason for the differences in insulin secretion might be the use of different diets.

The question whether the reduced blood glucose concentrations of $hadh^{-/-}$ mice are the result of the insufficient fuel consumption and/or the enhanced insulin secretion by the pancreas needs to be answered in the future. Our data indicate that hypoglycemia is due to a combination of both alterations. For the clarification of this question, it will be necessary to detect blood glucose and insulin concentrations, for instance, in the thermoneutral zone to avoid energy consumption for heat production. Another option could be to pair feed control and $hadh^{-/-}$ mice in a way that both mice would generate comparable amounts of ATP and reduction equivalents. Similar differences in glucose concentrations as in the previous experimental setting would indicate that it is the consequence of the higher insulin secretion.

In summary, our data indicate that inhibition of SCHAD reduces the body weight according to the excretion of acylcarnitines, which associates with a reduced fuel efficiency. It, furthermore, lowers blood glucose concentrations by elevating nutrient-stimulated insulin secretion.

Acknowledgments

We thank the skillful technical assistance of Andrea Teichmann, Daniel Bakó, and Henk van Lenthe; Ruben Rosenkranz for verification of GeneTrap mouse ES cells and for mouse genotyping; and Ingo Voigt for blastocyst injections.

Address all correspondence and requests for reprints to: Dr. A. Schürmann, Department of Experimental Diabetology, German Institute of Human Nutrition, Potsdam-Rehbruecke, Arthur-Scheunert-Allee 114-116, D-14558 Nuthetal, Germany. E-mail: schuermann@dife.de.

This work was supported by German Ministry of Education, Research, and Technology Grants 0313128B, NGFN2:01GS0487; NGFNplus:01GS0821; NEUROTARGET: 01GI0847; and DZD: 01GI0922.

Disclosure Summary: The authors have nothing to disclose.

References

1. **Schuler AM, Wood PA** 2002 Mouse models for disorders of mitochondrial fatty acid β-oxidation. ILAR J 43:57–65
2. **Roe CR, Ding J** 2001 Mitochondrial fatty acid oxidation disorders. In: Scriver C, Beaudet AL, Sly WS, Valle D., Childs B, Kinzler KW, Vogelstein B, eds. The metabolic and molecular bases of inherited disease, 8th ed. New York: McGraw-Hill; 2297–2326
3. **Hussain K, Blankenstein O, De Lonlay P, Christesen HT** 2007 Hyperinsulinaemic hypoglycaemia: biochemical basis and the importance of maintaining normoglycaemia during management. Arch Dis Child 92:568–570
4. **Eaton S, Chatziandreou I, Krywawych S, Pen S, Clayton PT, Hussain K** 2003 Short-chain 3-hydroxyacyl-CoA dehydrogenase deficiency associated with hyperinsulinism: a novel glucose-fatty acid cycle? Biochem Soc Trans 31:1137–1139
5. **Li C, Chen P, Palladino A, Narayan S, Russell LK, Sayed S, Xiong G, Chen J, Stokes D, Butt YM, Jones PM, Collins HW, Cohen NA, Cohen AS, Nissim I, Smith TJ, Strauss AW, Matschinsky FM, Bennett MJ, Stanley CA** 2010 Mechanism of hyperinsulinism in short-chain 3-hydroxyacyl-CoA dehydrogenase deficiency involves activation of glutamate dehydrogenase. J Biol Chem 285:31806–31818
6. **Plum L, Kluge R, Giesen K, Altmüller J, Ortlepp JR, Joost HG** 2000 Type 2 diabetes-like hyperglycemia in a backcross model of NZO and SJL mice: characterization of a susceptibility locus on chromosome 4 and its relation with obesity. Diabetes 49:1590–1596
7. **Kluge R, Giesen K, Bahrenberg G, Plum L, Ortlepp JR, Joost HG** 2000 Quantitative trait loci for obesity and insulin resistance (*Nob1, Nob2*) and their interaction with the leptin receptor allele (LeprA720T/T1044I) in New Zealand obese mice. Diabetologia 43: 1565–1572
8. **Giesen K, Plum L, Kluge R, Ortlepp J, Joost HG** 2003 Diet-dependent obesity and hypercholesterolemia in the New Zealand obese mouse: identification of a quantitative trait locus for elevated serum cholesterol on the distal mouse chromosome 5. Biochem Biophys Res Commun 304:812–817
9. **Vogel H, Nestler M, Rüschendorf F, Block MD, Tischer S, Kluge R, Schürmann A, Joost HG, Scherneck S** 2009 Characterization of Nob3, a major quantitative trait locus for obesity and hyperglycemia on mouse chromosome 1. Physiol Genomics 38:226–232
10. **Chadt A, Leicht K, Deshmukh A, Jiang LQ, Scherneck S, Bernhardt U, Dreja T, Vogel H, Schmolz K, Kluge R, Zierath JR, Hultschig C, Hoeben RC, Schürmann A, Joost HG, Al-Hasani H** 2008 Tbc1d1 mutation in lean mouse strain confers leanness and protects from diet-induced obesity. Nat Genet 40:1354–1359
11. **Ashrafi K, Chang FY, Watts JL, Fraser AG, Kamath RS, Ahringer J, Ruvkun G** 2003 Genome-wide RNAi analysis of *Caenorhabditis elegans* fat regulatory genes. Nature. 421:268–272
12. **Livak KJ, Schmittgen TD** 2001 Analysis of relative gene expression data using real-time quantitative PCR and the $2(-\Delta\Delta C(T))$ method. Methods 25:402–408
13. **Chace DH, Kalas TA, Naylor EW** 2003 Use of tandem mass spectrometry for multianalyte screening of dried blood specimens from newborns. Clin Chem 49:1797–1817
14. **Rashed MS, Ozand PT, Bucknall MP, Little D** 1995 Diagnosis of inborn errors of metabolism from blood spots by acylcarnitines and amino acids profiling using automated electrospray tandem mass spectrometry. Pediatr Res 38:324–331
15. **van Vlies N, Tian L, Overmars H, Bootsma AH, Kulik W, Wanders RJ, Wood PA, Vaz FM** 2005 Characterization of carnitine and fatty acid metabolism in the long-chain acyl-CoA dehydrogenase-deficient mouse. Biochem J 387:185–193
16. **Maeda Y, Ito T, Suzuki A, Kurono Y, Ueta A, Yokoi K, Sumi S, Togari H, Sugiyama N** 2007 Simultaneous quantification of acylcarnitine isomers containing dicarboxylic acylcarnitines in human serum and urine by high-performance liquid chromatography/elec-

trospray ionization tandem mass spectrometry. Rapid Commun Mass Spectrom 21:799–806
17. **Bartelt A, Bruns OT, Reimer R, Hohenberg H, Ittrich H, Peldschus K, Kaul MG, Tromsdorf UI, Weller H, Waurisch C, Eychmüller A, Gordts PL, Rinninger F, Bruegelmann K, Freund B, Nielsen P, Merkel M, Heeren J** 2011 Brown adipose tissue activity controls triglyceride clearance. Nat Med 17:200–205
18. **Henquin JC** 2009 Regulation of insulin secretion: a matter of phase control and amplitude modulation. Diabetologia 52:739–751
19. **Clayton PT, Eaton S, Aynsley-Green A, Edginton M, Hussain K, Krywawych S, Datta V, Malingre HE, Berger R, van den Berg IE** 2001 Hyperinsulinism in short-chain L-3-hydroxyacyl-CoA dehydrogenase deficiency reveals the importance of β-oxidation in insulin secretion. J Clin Invest 108:457–465
20. **Kurtz DM, Rinaldo P, Rhead WJ, Tian L, Millington DS, Vockley J, Hamm DA, Brix AE, Lindsey JR, Pinkert CA, O'Brien WE, Wood PA** 1998 Targeted disruption of mouse long-chain acyl-CoA dehydrogenase gene reveals crucial roles for fatty acid oxidation. Proc Natl Acad Sci USA 95:15592–15597
21. **Buchmann J, Meyer C, Neschen S, Augustin R, Schmolz K, Kluge R, Al-Hasani H, Jürgens H, Eulenberg K, Wehr R, Dohrmann C, Joost HG, Schürmann A** 2007 Ablation of the cholesterol transporter adenosine triphosphate-binding cassette transporter G1 reduces adipose cell size and protects against diet-induced obesity. Endocrinology 148:1561–1573
22. **Goetzman ES, Tian L, Wood PA** 2005 Differential induction of genes in liver and brown adipose tissue regulated by peroxisome proliferator-activated receptor-α during fasting and cold exposure in acyl-CoA dehydrogenase-deficient mice. Mol Genet Metab 84:39–47
23. **Molven A, Matre GE, Duran M, Wanders RJ, Rishaug U, Njølstad PR, Jellum E, Søvik O** 2004 Familial hyperinsulinemic hypoglycemia caused by a defect in the SCHAD enzyme of mitochondrial fatty acid oxidation. Diabetes 53:221–227
24. **Leiter EH** 2002 Mice with targeted gene disruptions or gene insertions for diabetes research: problems, pitfalls, and potential solutions. Diabetologia 45:296–308
25. **Coleman DL** 1978 Obese and diabetes: two mutant genes causing diabetes-obesity syndromes in mice. Diabetologia 14:141–148
26. **Beisel WR** 1982 Single nutrients and immunity. Am J Clin Nutr 35:417–468